Correlation of Vibrational and Electronic Spectra. 2. Static and Vibronic Contributions to the Polarized Spectrum of Trisethylenediaminenickel(II) Dinitrate

Adam J. Bridgeman, Kathleen M. Jupp, and Malcolm Gerloch*

University Chemical Laboratories, Cambridge University, Lensfield Road, Cambridge CB2 1EW, UK

Received November 5, 1993[⊗]

The transition energies and intensity distributions in both linearly and circularly polarized spectra of $[Nien_3][NO_3]_2$ have been reproduced quantitatively within the cellular ligand-field model. In addition to the Racah B parameter for the interelectron repulsion energies, transition energies required only one ligand-field parameter. Following a normal coordinate analysis of vibrational frequencies, the relative intensities of five observed bands in linear polarization and of three bands in the crystal axial circular dichroism spectrum have been reproduced subsequently with just one variable. The absolute magnitude of the rotatory strength or, equivalently, the intensity of the CD spectrum relative to the linearly polarized spectrum is reproduced within 17% of one experimental estimate; however, two independent experimental measures of this quantity differ by nearly a factor of 4. It is shown that even that difference can be accounted for on recognition of a small contribution from bent bonding in this complex.

Introduction

Our studies of the intensity distribution in the "d−d" spectra of transition metal complexes began with a model[1] for the analysis of acentric chromophores whose intensity derives from parity mixing within the static environment. The approach was tested and exploited in part II[2] of that series; excellent reproduction of the relative intensities of the spectra of various tetrahedral and trigonal bipyramidal complexes was achieved. Included in the test systems at that time was the spectrum of the trisethylenediaminenickel(II) cation. Though not centrosymmetric, the coordination in this complex approaches octahedral somewhat and it was therefore no surprise to find that our "static" model of intensities failed utterly to reproduce the experimental traces. Indeed, this "failure" was considered to be a success in demonstrating that the static model could not be manipulated to reproduce experiment in circumstances in which vibronically induced parity mixing might be expected to be important.

In part IV[3] of this series of intensity studies, we introduced a vibronic or "dynamic" model for the spectral analysis of centric chromophores. Free variables are associated with each vibrational mode. Analyses with so high a degree of parameterization were difficult, but it was possible to correlate[4,5] the intensity distributions in planar $CuCl_4^{2-}$ and PtX_4^{2-} (X = Cl, Br) with their quite different vibrational frequencies. $[Nien_3][NO_3]_2$ crystallizes[6] in the hexagonal class. The polarized, single crystal d−d spectrum[7] is characterized by three spin-allowed transitions in each of the two unique polarizations but the highest energy transition is masked by the charge-transfer spectrum in the ∥ c polarization. So experiment provides only five pieces of data, equivalent to just four relative intensities. The problems of their analysis within our original vibronic model[3] are obvious. First, errors arise if the normal modes differ significantly from the symmetry modes for the total calculated intensity is given as a sum of intensities from each vibration mode and not as the square of the (vectorial) sum of the transition moments. This procedure is correct for independent vibrations but is not "self-correcting" if the normal modes are incorrectly defined. Second, the problem is grossly underdetermined if parameters for different vibrations are totally free. Third, the latter problem is made even worse if there are no relationships between vibrational parameters and static ones, for one must expect significant contributions from both sources of parity mixing in this chromophore.

All the problems vanish, in principle, using the extended version of our vibronic model, described in the preceding paper.[8] Here the vibronic modeling is predicated upon a full normal coordinate analysis of the vibrational, infrared frequencies. The normal modes are thus determined in detail so that not only are ligand displacements known in the various independent vibrations, so relating the vibronic intensity parameters of one mode to another, but that the ratios of vibronic parameters to static parameters are also known. All ${}^{L}t^{\alpha}_{\lambda}(Q)$ parameters, as defined in the preceding paper, are thus expressed in terms of the "static" parameters ${}^{L}t_{\lambda}$. The mechanics are thus factored out of the analysis and there remain only electronic or bonding variables. As no direct π interaction is envisaged between metal and ethylenediamine ligands, $\lambda = \sigma$ only. There is only one donor atom type. This system is ideal, therefore, in requiring only two intensity parameters to define the spectrum—${}^{P}t_{\sigma}$ and ${}^{F}t_{\sigma}$. However, we may only determine *relative* intensities, so that we employ just *one* intensity variable in this case. It is, of course, very interesting to see whether so exacting a test of the model is successful.

In addition to this interest in the electric dipole strengths in the $[Nien_3]^{2+}$ ion is one in the rotatory strengths as measured by circular dichroism. The molecular symmetry of the $[Nien_3]^{2+}$ ion is D_3 and chiral; the complex spontaneously resolves on crystallization. Yang and Palmer[9] and Harding et al.[10] have independently reported single crystal, axial CD spectra for this complex. The rotatory strength arises theoretically[10] only from

[⊗] Abstract published in *Advance ACS Abstracts,* October 15, 1994.

(1) Brown, C. A.; Gerloch, M.; McMeeking, R. F. *Mol. Phys.* **1988**, *64*, 771.
(2) Brown, C. A.; Duer, M. J.; Gerloch, M.; McMeeking, R. F. *Mol. Phys.* **1988**, *64*, 793.
(3) Duer, M. J.; Essex, S. J.; Gerloch, M.; Jupp, K. M. *Mol. Phys.* **1993**, *79*, 1147.
(4) Duer, M. J.; Essex, S. J.; Gerloch, M. *Mol. Phys.* **1993**, *79*, 1167.
(5) Bridgeman, A. J.; Gerloch, M. *Mol. Phys.* **1993**, *79*, 1195.
(6) Korp, J. D.; Bernal, I.; Palmer, R. A.; Robinson, J. C. *Acta Crystallogr.* **1980**, *36B*, 560.
(7) Dingle, R.; Palmer, R. A. *Theor. Chim. Acta (Berlin)* **1966**, *6*, 249.
(8) Bridgeman, A. J.; Essex, S. J.; Gerloch, M. *Inorg. Chem.*, preceding paper in this issue.
(9) Yang, M. C.-H.; Palmer, R. A. *J. Chin. Chem. Soc.* **1978**, *26*, 195.

0020-1669/94/1333-5424$04.50/0

the "static" sources of parity mixing and not from the vibronic. It is of obvious interest to see whether the parameterization that can reproduce the linearly polarized spectrum can account for the circularly polarized one also.

Normal Coordinate Analysis

The calculation of the intensity in the ligand-field spectrum of the $[Nien_3]^{2+}$ ions derived from vibronic coupling requires a prior normal coordinate analysis of the vibrational frequencies. The chelation and inherent complexity of the ethylenediamine ligand means that the normal modes of the ion are intimate mixtures of many energetically similar local motions. Use of symmetry modes based on the skeletal vibrations of the NiN_6 unit is unlikely to represent adequately the true normal modes. A normal coordinate analysis also allows the calculation of ligand angular displacements at the temperature of interest. This effectively removes the dynamic part of the vibronic coupling calculations.

There have been a number of reported studies[11-15] of the vibrational spectra of metal−ethylenediamine complexes. The most detailed by Borch et al.[13-15] concerned the vibrational characteristics of the $[Rhen_3]^{3+}$ ion. Their study included a normal coordinate analysis of the infrared (IR) and Raman spectra of this ion and seven isotopically labeled species. However, Borch et al. were apparently unaware of the crystallographically determined molecular geometry of this ion and built their structure using assumed ligand dimensions and octahedral coordination around the metal.

We have repeated calculations using the force constants reported by Borch et al. but employing the molecular geometry[16] and ligand conformation reported for the $[Rhen_3]^{3+}$ ion in the active racemate $[(+)\text{-}Cren_3(+)\text{-}Rhen_3]Cl_6$. While for many of the normal modes fit with experimental frequencies was reasonable, two regions of the spectra were poorly reproduced. Vibrations involving motion of the carbon- and nitrogen-bound hydrogen atoms were calculated to be too high in energy. This can be related to the poor choice of angles and lengths for bonds involving hydrogen by Borch et al.

The second region of poor fit was in the low-energy part of the spectrum. It is this region that contains the vibrations of the RhN_6 unit of most interest in the present study. The poor match with experiment is directly related to the approximations used in the molecular geometry. In all normal coordinate calculations described below, the crystallographically determined geometries have been used. The D_3 molecular symmetry has been exploited in the definitions of the internal coordinate force constants.

The IR spectrum of the $[Nien_3]^{2+}$ ion has been reported.[17] Unfortunately only vibrations of A_2 and E symmetry are IR active. The remaining A_1 modes are Raman active only. It has not then been possible to fit every calculated mode to an observed frequency. For the $[Rhen_3]^{3+}$ system, however, Borch et al. have reported and assigned full IR and Raman spectra.

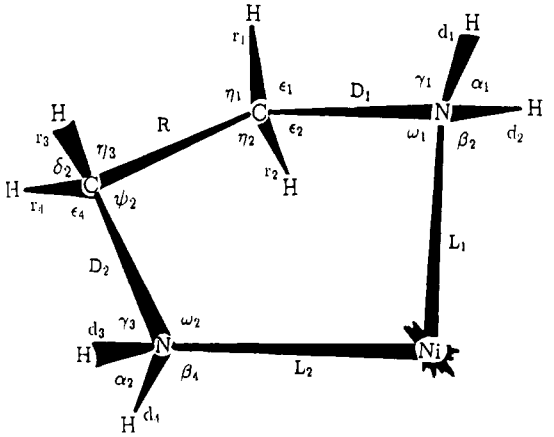

Figure 1. Internal coordinates of the chelate ring. Greek symbols label bends; Roman symbols label stretches and atoms. Additional coordinates are as follows: torsion around the Ni−N bonds τ_1 and τ_2; torsion around the N−C bonds, π_1 and π_2; torsion around the C−C bond, Δ.

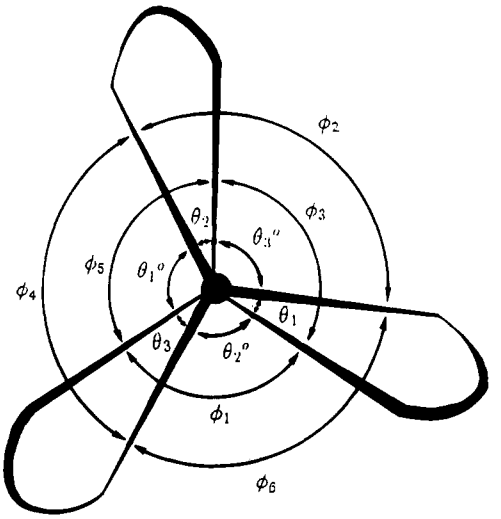

Figure 2. Internal bend coordinates of the NiL_6 unit.

In the normal coordinate analysis of the $[Nien_3]^{2+}$ system, the following method has been employed. First, using the force constants reported by Borch et al. as starting values, a rough fit for the $[Rhen_3]^{3+}$ ion, with geometry defined by the Cr−Rh racemate above, was obtained by variation of the minimum number of force constants. For the $[Nien_3]^{2+}$ ion, assignments were then made on the basis of calculations referred to the true $[Nien_3]^{2+}$ geometry,[6] using these force constants; the geometries, experimental frequencies, and so presumably the normal modes of the two complexes are similar. Finally, the force constants were refined as outlined below. To the best of our knowledge, the present study represents the first vibrational analysis of a $[Men_3]$ system with no approximations as regards geometry.

All calculations use Wilson's GF matrix method[18] with an internal coordinate basis set and have been performed using our normal coordinate analysis program[19] and a modified general valence force field (GVFF).[20] The $[Nien_3]^{2+}$ system characterizes a 37-body problem. The 138 internal coordinates required for a complete description of the possible vibrational motions are shown in Figures 1 and 2. The 105 ($=3N - 6$) normal modes transform as $18A_1 + 17A_2 + 35E$ under the D_3 point

(10) Harding, M. J.; Mason, S. F.; Peart, B. J. *J. Chem. Soc., Dalton Trans.* **1973**, 955.
(11) Ashley, P. J.; Torrible, E. G. *Can. J. Chem.* **1969**, *47*, 167.
(12) Omura, Y.; Nakagawa, I.; Shimanowski, T. *Spectrochim. Acta* **1971**, *27A*, 2227.
(13) Borch, G.; Nielson, P. H.; Klaeboe, P. *Acta Chem. Scand.* **1977**, *31A*, 109.
(14) Borch, G.; Klaeboe, P.; Nielson, P. H. *Spectrochim. Acta* **1978**, *34A*, 87.
(15) Borch, G.; Gustaven, J.; Klaeboe, P.; Nielson, P. H. *Spectrochim. Acta* **1978**, *34A*, 93.
(16) Whuler, A.; Brouty, C.; Spirat, P.; Herpin, P. *Acta Crystallogr.* **1976**, *32B*, 2542.
(17) Bennett, A. M. A.; Foulds, G. A.; Thornton, D. A.; Watkins, G. M. *Spectrochim. Acta* **1990**, *46A*, 13.
(18) Wilson, E. B., Jr.; Decius, J. C.; Cross, J. C. *Molecular Vibrations*; McGraw-Hill: New York, 1955.
(19) Bridgeman, A. J.; Gerloch, M. VANAL, a FORTRAN computer program, 1993.
(20) Califano, S. *Vibrational* States; Wiley-Interscience: New York, 1976.

Table 1. Calculated and Observed Vibrational Frequencies

ν_{calc}/cm^{-1}	ν_{obs}/cm^{-1}	symm	PED[a] and symmetry mode breakdown[b,c]	ν_{calc}/cm^{-1}	ν_{obs}/cm^{-1}	symm	PED[a] and symmetry mode breakdown[b,c]
119	120	E	τ_{as}NC(15), τ_{as}NiN(45), δNNiN(37)	1097		A_1	ν_sCN(12), tCH$_2$(35), νCC(28)
			[60% S_6, 20% S_7, 20% S_8]	1126	1111	A_2	δCH$_2$(35), ωCH$_2$(32), tCH$_2$(18)
142	141	A_2	τ_{as}NC(12), τ_{as}NiN(54), δNNiN(18)	1127	1111	E	δCH$_2$(54), ωCH$_2$(32)
			[100% S_4]	1150	1152	E	δCH$_2$(43), ωCH$_2$(39)
197	200	E	δNNiN(75), τ_s NC(6)	1150		A_1	δCH$_2$(39), ωCH$_2$(41)
			[10% S_6, 45% S_7, 45% S_8]	1256	1274	E	δCH$_2$(80), ωCH$_2$(5), ωNH$_2$(5)
235	234	A_2	δNNiN(42), τ_{as}NC(8), τCC(12)	1257		A_1	δCH$_2$(80), ωNH$_2$(5)
			[100% S_4]	1292	1297	E	δCH$_2$(65), ωNH$_2$(8), ωCH$_2$(8)
275		A_1	ν_sNiN(48), δNiNC(16), δNNiN(18)	1293	1297	A_2	δCH$_2$(70), ωCH$_2$(12), ωNH$_2$(12)
			[20% S_1, 75% S_2, 5% S_3]	1326	1327	E	tNH$_2$(64), δNH$_2$(15), δCH$_2$(21)
288	284	E	ν_sNiN(35), δNNiN(42), τ_sNiN(20)	1326	1327	A_2	tNH$_2$(70), δNH$_2$(15), δCH$_2$(10)
			[6% S_5, 46% S_6, 24% S_7, 24% S_8]	1327	1327	E	tNH$_2$(70), δNH$_2$(18)
319	324	E	ν_sNiN(22), δNiNC(12), τ_sNC(18), δNNiN(12)	1330		A_1	tNH$_2$(75), δNH$_2$(10)
			[12% S_5, 20% S_7, 34% S_7, 34% S_8]	1361	1368	A_2	δCH$_2$(95)
330		A_1	ν_sNiN(21), δNNiN(47), τ_sNiN(18), δNiNC(12)	1364	1368	E	δCH$_2$(95)
			[100% S_3]	1390	1391	E	δNH$_2$(60), tNH$_2$(28)
366		A_1	δNCC(12), τCC(10), δNNiN(36), δNiNC(10)	1392		A_1	δNH$_2$(62), tNH$_2$(20), δCH$_2$(10)
			[7% S_1, 50% S_2, 43% S_3]	1454	1455	E	δNH$_2$(30), tNH$_2$(62)
401	403	E	ν_{as}NiN(48), νCC(10), δNiNC(18), δNNiN(19)	1455	1455	A_2	δCH$_2$(30), tNH$_2$(50)
			[64% S_5, 20% S_6, 8% S_7, 8% S_8]	1459	1461	E	δNH$_2$(20), tNH$_2$(46), δCH$_2$(20)
499	499	E	ν_{as}NiN(36), δNCC(15), δNNiN(10)	1460		A_1	δNH$_2$(20), tNH$_2$(39), δCH$_2$(10)
			[35% S_5, 45% S_6, 10% S_7, 10% S_8]	1588	1590	A_2	δNH$_2$(95)
507	499	A_2	ν_{as}NiN(35), δNCC(18), δNNiN(6)	1590	1590	E	δNH$_2$(95)
			[100% S_4]	1597	1605	E	δNH$_2$(94)
526	523	E	ν_{as}NiN(24), νCC(39), δNiNC(14), δNCC(12)	1600		A_1	δNH$_2$(94)
533		A_1	νCC(45), δNiNC(25), δNCC(8)	2883	2886	A_2	ν_sCH(98)
647	663	A_2	ϱNH$_2$(36), δNCC(34), δNiNC(8), ϱCH$_2$(12)	2884	2886	E	ν_sCH(99)
667	663	E	ϱNH$_2$(34), δNCC(30), δNiNC(8), ϱCH$_2$(18)	2888	2886	E	ν_sCH(99)
708	720	E	ϱNH$_2$(82), νCC(10)	2889		A_1	ν_sCH(100)
721		A_1	ϱNH$_2$(81), νCC(10)	2944	2947	A_2	ν_sCH(100)
769	775	E	ϱNH$_2$(85), ϱCH$_2$(5)	2944	2947	E	ν_sCH(100)
788	775	A_2	ϱNH$_2$(83), ϱCH$_2$(7)	2949	2947	E	ν_{as}CH(100)
887	864	E	ν_sCN(54), νCC(11), ϱCH$_2$(24)	2950		A_1	ν_{as}CH(100)
888	876	A_2	ν_sCN(52), νCC(11), ϱCH$_2$(22)	3170	3171	A_2	ν_sNH(100)
969		A_1	ν_sCN(18), ϱCH$_2$(50), ϱNH$_2$(10)	3171	3171	E	ν_sNH(100)
973	983	E	ν_{as}CN(63), ϱCH$_2$(26)	3171	3171	E	ν_sNH(100)
1023	1016	A_2	ν_{as}CN(20), νCC(40), ϱNH$_2$(10), tCH$_2$(12)	3171		A_1	ν_sNH(100)
1026	1023	E	ν_{as}CN(16), tCH$_2$(11), νCC(38), ϱNH$_2$(10)	3267	3243	A_2	ν_{as}NH(100)
1077		A_1	ν_sCN(18), tCH$_2$(31), νCC(30)	3267	3243	E	ν_{as}NH(100)
1078	1075	E	ν_{as}CN(12), tCH$_2$(21), νCC(30)	3267	3243	E	ν_{as}NH(100)
1093	1091	E	ν_{as}CN(21), tCH$_2$(33), νCC(32)	3267		A_1	ν_{as}NH(100)

[a] Defined as $x_{ik} = 100 f_{ii} L_{ik}^2/\lambda_k$, where **F** is the force constant matrix, **L** is the eigenvector matrix, and λ_k are the diagonal elements of the eigenvalue matrix Λ in the secular equation[18] **GFL** = **L**Λ. [b] Symmetry coordinates involving NNiN deformation. A_1: $S_1 = (\theta_1 + \theta_2 + \theta_3)/3^{1/2}$; $S_2 = (\theta_1^0 + \theta_2^0 + \theta_3^0)/3^{1/2}$; $S_3 = (\phi_1 + \phi_2 + \phi_3 + \phi_4 + \phi_5 + \phi_6)/6^{1/2}$. A_2: $S_4 = (\phi_1 - \phi_2 + \phi_3 - \phi_4 + \phi_5 - \phi_6)/6^{1/2}$. E: S_5(i) $= (2\theta_1 - \theta_2 - \theta_3)/6^{1/2}$; S_6(i) $= (2\theta_1^0 - \theta_2^0 - \theta_3^0)/6^{1/2}$; S_7(i) $= (2\phi_1 - \phi_3 - \phi_5)/6^{1/2}$; S_8(i) $= (2\phi_2 - \phi_4 - \phi_6)/6^{1/2}$; S_5(ii) $= (\theta_2 - \theta_3)/2^{1/2}$; S_6(ii) $= (\theta_2^0 - \theta_3^0)/2^{1/2}$; S_7(ii) $= (\phi_3 - \phi_5)/2^{1/2}$; S_8(ii) $= (\phi_4 - \phi_6)/2^{1/2}$. [c] Key to symbols: ν, stretch; δ, deformation; ϱ, rock; ω, wag; t, twist; τ, torsion; subscript s, symmetric; subscript as asymmetric. Full descriptions of local chelate ring motions given by Borch et al.[13]

group. The redundancies were eliminated by the analysis. The number of interaction force constants has been kept at a minimum by neglecting those which have a small influence on the calculated frequencies. We have found that the force field can be described adequately using 40 force constants, of which 23 are interaction terms.

The potential energy distribution (PED) of the normal modes among each of the internal coordinates has been used extensively in the analysis. This is defined in Table 1 and is a convenient way of estimating the significant force constants for each vibration. By this means, restricted regions of the spectrum were fitted in turn by the variation of a small number of force constants. This was particularly useful in the analysis of relatively uncoupled motions, such as those involving the hydrogen atoms. Final fitting employed rather larger groups of force constants and included the use of least-squares refinement.

The optimal fit to experiment is given in Table 1. This also includes an approximate description of the vibrations using the PED. The vibrations of most interest in the present study are those containing significant amounts of N−Ni−N bends. These occur in the low-energy region of the spectrum, below 400 cm^{-1}. The bending components of these modes are shown in the table as further broken down in terms of the symmetry modes of the NiN_6 fragment. Both of these descriptions of the normal modes illustrate the degree of mixing and complexity of these vibrations. It is hardly surprising that symmetry modes cannot adequately represent the normal modes in ligand-field intensity calculations.

The optimal force constants are given in Table 2. Force constants related to the ethylenediamine ligand are comparable with those reported[20−25] in similar molecules. Significant differences are observed for motions involving the amino groups, which we presume reflect complexation to the nickel cation. For an aliphatic amine, for example, the N−H stretch force

(21) Snyder, R. G.; Schachtschreider, J. H. *Spectrochim. Acta* **1965**, *21*, 169.
(22) Schachtschneider, J. H.; Snyder, R. G. *Spectrochim. Acta* **1963**, *19*, 168.
(23) Dellepiane, G.; Zerbi, G. *J. Chem. Phys.* **1968**, *48*, 3573.
(24) Griffith, W. P. *J. Chem. Soc. A* **1966**, 899.
(25) Bigotto, A.; Costa, G.; Galosso, V.; De Alti, G. *Spectrochim. Acta* **1970**, *26A*, 1939.

Table 2. Optimal Force Constants

force type	group	coordinates involved	atoms common to interacting coordinates	optimal value[a]
stretch	NiN_6	Ni−N		1.760
	NH_2	N−H		5.721
	CH_2	C−H		4.628
	CH_2−CH_2	C−C		3.978
	CH_2−NH_2	C−N		4.664
stretch−stretch	NiN_6	Ni−N, Ni−N (cis; on same ring)	Ni	−0.167
	NiN_6	Ni−N, Ni−N (cis; on different rings)	Ni	−0.048
	NiN_6	Ni−N, Ni−N (trans)	Ni	0.309
	NH_2	N−H, N−H	N	−0.112
	CH_2	C−H, C−H	C	0.007
	CH_2−CH_2−NH_2	C−C, C−N	C	0.091
bend	NiN_6	∠N−Ni−N		
	CH_2	∠H−C−H		0.341
	NH_2	∠H−N−H		0.302
	CH_2−CH_2	∠C−C−H		0.502
	CH_2−NH_2	∠H−C−N		0.973
	CH_2−NH_2	∠C−N−H		0.351
	CH_2−CH_2−NH_2	∠C−C−N		1.832
	NH_2−Ni	∠H−N−Ni		0.338
	CH_2−NH_2−Ni	∠C−N−Ni		1.565
bend−bend	CH_2−CH_2	∠H−C−C, ∠H−C−C	C−C	−0.147
	CH_2−NH_2	∠H−C−N, ∠H−C−N	C−N	−0.037
	NH_2−Ni	∠H−N−Ni, ∠H−N−Ni	N−Ni	0.021
	CH_2−CH_2	∠H−C−C, ∠C−C−H	C−C	0.131
	NiN_6	∠N−Ni−N, ∠N−Ni−N (right angles)	Ni−N	0.250
	NiN_6	∠N−Ni−N, ∠N−Ni−N (coplanar)	Ni−N	−0.440
	NiN_6	∠N−Ni−N, ∠N−Ni−N (trans)	Ni	−0.160
stretch−bend	CH_2−CH_2	C−C, ∠H−C−C	C−C	0.450
	CH_2−CH_2−NH_2	C−C, ∠H−C−N	C	−0.053
	CH_2−CH_2−NH_2	C−C, ∠C−C−N	C−C	−0.500
	CH_2−NH_2	C−N, ∠C−N−H	C−N	0.340
	CH_2−NH_2	C−N, ∠H−C−N	C−N	0.049
	CH_2−CH_2−NH_2	C−N, ∠H−C−C	C	−0.098
	CH_2−CH_2−NH_2	C−N, ∠C−C−N	C−N	0.700
	Ni−NH_2−CH_2	Ni−N, ∠Ni−N−C	Ni−N	0.023
	Ni−NH_2−CH_2	C−N, ∠Ni−N−C	C−N	−0.204
torsion	CH_2−NH_2−Ni−NH_2	Ni−N		0.216
	Ni−NH_2−CH_2−CH_2	N−C		0.054
	NH_2−CH_2−CH_2−NH_2	C−C		0.100

[a] Units: stretch, mdyn/Å; stretch−bend, mdyn/rad; bend and bend−bend, mdyn Å/(rad)^2; torsion, mdyn Å/(rad)^2.

constant has been found[26] to be approximately 6.4 mdyn/A. For the present system, it is found somewhat lower at approximately 5.7 mdyn/A. The value reported here for N−C torsion is considerably higher than that for free amines,[23] a stiffening presumably resulting from chelation. There is less precedent for the values obtained for the skeletal vibrations in the NiN_6 unit. The Ni−N stretch force constant is comparable to that found for the Rh−NH_3 bond.[24]

There is significant NiN_6 bend contribution only to the 10 lowest energy vibrations. For each of these, ligand angular displacements at 25 K with respect to defined local axes have been calculated. At this temperature, the normal modes are expected to be harmonic and the calculated displacements are found to be small as required by the vibronic intensity model. The following CLF intensity analysis is based upon the tangential ligand displacements for all the lowest energy vibrations; that is, bond elongations or compressions have been neglected.

Ligand-Field Analyses

Transition Energies. With no discernable differences between the spectral band maxima in σ and π ($\perp$ c and $\parallel$ c) polarizations,[9] we seek to reproduce just three transition energies. The molecular structure[6] of the $[Nien_3]^{2+}$ ion possesses strict D_3 symmetry so all amine donors are rigorously equivalent. Within the cellular ligand-field (CLF) model, their local ligand fields are parameterized with e_σ alone. All computations have been performed using the CAMMAG4 program suite[27] within the spin-triplet basis of d^8, $^3F + {}^3P$. Interelectron repulsion effects are parameterized with the Racah B variable and spin−orbit coupling with the one-electron coefficient, ζ. Neither energy nor intensity analyses could define the magnitude of ζ more exactly than ± 100 cm^{-1} of the value 550 cm^{-1} that was otherwise held fixed throughout all the following procedures. (The free-ion value is $\zeta_0 = 630$ cm^{-1}.) Wide variation of the remaining two variables, B and e_σ, yielded a good and essentially unique fit to the three experimental transition energies. Comparison of observed transition energies with those optimally calculated with the values $B = 870$ cm^{-1} and $e_\sigma = 4010$ cm^{-1} is made in Table 3; the corresponding ligand-field trace, Σ, is 24 060 cm^{-1}.

Intensities. Two well-resolved bands are present in each of the two crystal polarizations. In addition, the highest energy band is reasonably resolved from an intense charge-transfer absorption in the σ spectrum. Estimates for five band areas are thus to be reproduced by the CLF intensity model. As no Ni−N π interactions are envisaged, we might consider $^Pt_\sigma$, $^Ft_\sigma$, and $^Rt_\sigma$ variables. However, as described in the original "static" model,[1] contributions from $^Rt_\sigma$ parameters in chromophores with bipyramidal or antibipyramidal geometries vanish identically.

(26) Lusser, R.; Edwards, J. O.; Eisenberg, R. *Inorg. Chim. Acta* **1969**, *3*, 468.

(27) Dale, A. R.; Duer, M. J.; Fenton, N. D.; Gerloch, M.; McMeeking, R. F. CAMMAG4, a FORTRAN computer program, 1991.

Table 3. Observed and Calculated d−d Transition Energies from $^3A_2$ Ground State

obsd/cm^{-1}	calcd/cm^{-1}	symmetry	
29 760	30 127	^3E	
			[$^3T_{1g}$(P)]
	29 070	$^3A_2$	
18 940	19 350	$^3A_2$	
			[$^3T_{1g}$(F)]
18 620	18 281	^3E	
11 630	11 966	$^3A_1$	
			[$^3T_{2g}$(F)]
	11 653	^3E	

Table 4. Comparison of Observed and Calculated Intensities[a]

	intensity distribution					
	σ		π		CD axial	
band/cm^{-1}	obsd	calcd	obsd	calcd	obsd	calcd
9000−15000	24.2	23.0	30.1	30.6	−957	−952
15000−24000	18.6	20.7	9.9	10.2	−36	−42
28000−32000	17.3	15.5	*b*	7.9	−7	−6

[a] To convert intensity to absolute units multiply by 6.06 D^2 cm^{-1}. To convert observed CD to absolute units multiply by 3.77 D μ_B cm^{-1}. To convert calculated CD to absolute units multiply by 3.02 D μ_B cm^{-1}. Calculations in absolute units require intensity parameters $^Pt_\sigma = 0.160$ D and $^Ft_\sigma = 0.040$ D. Negative signs of CD bands are associated with $\Delta(\lambda\lambda\lambda)$ configuration. [b] Transition obscured by charge-transfer feature.

Table 5. Relative Contributions from Static and Vibronic Sources to the Linearly Polarized Spectrum

	intensity contribution[a]			
	σ		π	
band/cm^{-1}	static	vibronic	static	vibronic
9000−15000	4.9	18.1	19.4	11.2
15000−24000	12.2	8.5	0.1	10.1
28000−32000	9.1	6.4	0.0	7.9

[a] To convert intensity to absolute units multiply by 6.06 D^2 cm^{-1}.

Further, since we address intensity *distributions*, or *relative* intensities, rather than absolute intensities, there remains just the ratio $^Pt_\sigma/^Ft_\sigma$ as the only intensity variable in this system. The relative contributions to intensity from different vibrations or from the static environment have been fixed by the preceding normal coordinate analysis of vibration frequencies. With $^Pt_\sigma$ fixed at 100 (arbitrary units), $^Ft_\sigma$ was varied from 0 to 2000. A unique and excellent fit to the relative experimental band areas was found for $^Ft_\sigma = 25 \pm 15$. The fit was found in ca. 30 s of computing time within the CAMMAG4 system. Subsequent least-squares refinement took some 4 min on our SUN Sparc IPC Workstation. Many hours had been spent on this analysis within the original[3] vibronic model in which different symmetry modes were freely parameterized without prior normal coordinate analysis; the results were highly ambiguous and, because of our ignorance of the detailed differences between the normal and symmetry modes, incorrect. The present analysis was thus pleasingly simple, unambiguous, and direct. Table 4 compares the observed relative intensities with those calculated by the optimal *P*/*F* ratio (100/25) above. Table 5 shows the relative contributions to the intensities deriving from the static environment and from all bending vibrations. These vary in detail from band to band; overall, however, we note that static and dynamic sources of parity mixing are roughly equal generators of intensity in this chromophore.

Circular Dichroism. Although $Nien_3(NO_3)_2$ spontaneously resolves on crystallization, the optical activity of neither enantiomer is retained on subsequent dissolution. Circular dichroism has therefore been measured for this chromophore in the solid state. Single crystal, axial CD spectra have been recorded independently by two research groups.[9,10] One has also performed an X-ray crystallographic analysis[6] using the Bijvoet method to establish an unambiguous correlation between the sign of optical rotation and structural handedness. There is good agreement between the distributions of optical rotation among the spin-allowed bands reported by the two research groups. There is considerable disagreement, however, with respect to the absolute magnitudes of the rotary strengths. The lowest energy band displays the greatest optical activity by far with a differential extinction coefficient, $|\Delta\epsilon| = |\epsilon_L - \epsilon_R|$, of ca. 6 by Yang and Palmer,[9] but of only ca. 3 by Harding et al.[10] There is a roughly similar disparity of the linear extinction coefficients between these two reports such that the ratio $|\Delta\epsilon/\epsilon|$ differs by nearly a factor of 4. Obtaining suitable crystals of even thickness, let alone the measurement of that thickness, is well-known to be difficult; we must presume that such problems underly these quantitative uncertainties.

Our analysis of the CD began, therefore, by addressing the qualitative pattern of differential extinctions that appears to be well established. That pattern is well reproduced by the optimal $\{e\}$ and $\{t\}$ parameter sets described above. In other words, the CD distribution was quantitatively reproduced simultaneously with the linear intensity distributions without further variables. The agreement is shown in Table 5.

Absolute rotatory strengths are calculated within our model as follows. Absolute values of the ^Lt parameters are established, after optimization of the intensity distribution, by scaling to the absolute experimental intensities. Thereafter, circular dichroism is calculated without further scaling and compared directly with experiment. The only variable for adjustment of calculated $\Delta\epsilon$ values is the orbital reduction factor k in the magnetic moment operator, $kl_\alpha + 2s_\alpha$; $\alpha = x, y, z$. The optical activity is found to vary nearly linearly with k, as is to be expected theoretically of an essentially space- (rather than spin-) determined property. A typical k value might be 0.9; it is not expected to lie outside the range 0.7−1.0 in the present complex. With k at its maximum value of 1.0, we compute the rotatory strengths of the present complex to be some 17% less than that reported by Yang and Palmer.[9] Given the manifest experimental difficulties of scaling (but not of distribution), this might be considered to be satisfactory agreement. On the other hand, a k value of ca. 0.25 would be required to reproduce the optical activity reported by Harding et al.[10] So low a value for k is unacceptable. Even given the experimental uncertainty, we have considered refinements of the ligand field that allow this issue to be resolved.

These arise from a consideration of the origins of the chirality in this (or other) chromophore. In Figure 3a we show a view of the molecule down the threefold rotation axis; triangles are drawn to associate donor atoms related by this triad. If we focus exclusively upon the first coordination shell, the twist of these triangles from the perfectly staggered configuration of O_h symmetry (or, of course, from the eclipsed one of D_{3h}) is responsible for the overall molecular chirality. The lower, D_3, symmetry allows, but does not cause, the optical activity in this system. Ultimately the cause lies in the details of the electron density distribution about the metal, so that the necessary lack of an improper symmetry axis is not enough. A zeroth order view of the electron density in this molecule is one of bonding electrons being concentrated along the Ni−N line of centers. Indeed such a view is built into the CLF calculations reported above. A more refined view, however, indicates that bonding density is expected to be displaced somewhat from these lines of centers for the Ni−N bonds to be bent. The bending should occur in two ways, as illustrated in Figure 3b,c. Figure 3b

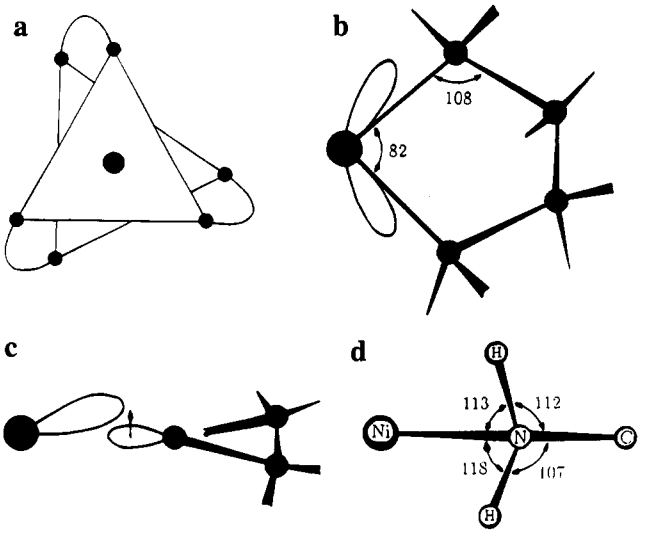

Figure 3. Origins of misdirected valence in $[Ni(en)_3]^{2+}$. Key: (a) D_3 global symmetry; (b) chelate ring strain; (c) metal orbital misalignment due to D_3 symmetry and twisting; (d) coordination geometry around the chelate nitrogen implies orbital displacement indicated by the arrow in (c); see text.

illustrates one chelation in a plane containing the nickel and two nitrogens; Figure 3c views the same chelation onto the plane normal to that in (b). The angle Ni−N−C of 108°, being close to the ideal tetrahedral angle, suggests that the amine donor lone pair is fairly accurately directed toward the metal atom. On the other hand, the metal is engaged in the bonding of six donor atoms. Close to the metal core, that bonding electron density will tend very strongly to gather in a strict octahedral manner so as to minimize interelectron repulsions whose importance is of prime concern in the small volume near the core. Further out from the core, overlap increases in importance and we expect compromises that lead to bent bonding. In Figure 3b we sketch the misdirected valence arising, in effect, from ring strain while, in (c) we show a similar misalignment arising from the overall twisting illustrated in (a). As described elsewhere,[28] the resulting lowering of local Ni−N pseudosymmetry is parameterized within the CLF approach with local off-diagonal ligand-field matrix elements, $e_{\sigma\pi}$; there is ample evidence of the efficacy of this approach. A more detailed view yet is generated from a study of the coordination geometry about the donor nitrogens, shown in Figure 3d. The implication of the inequality of the Ni−N−H angles or of the C−N−H angles is that the nitrogen lone pair is not ideally directed at the metal atom as in the first-order view above but toward points somewhat "in front" of the nickel. The suggested orbital displacement is indicated by the arrow in Figure 3c.

All of these orbital misalignments are such as to place the bonding electron density around the nickel atom in regions that are less displaced from octahedral that those indicated by consideration of the donor atom locations alone. In other words, the electronic chirality in this chromophore is somewhat less than the nuclear chirality; the electron density is "dragged" away from the ideal octahedron by the chelation and twisted nuclear ligation, but incompletely so.

(28) Duer, M. J.; Fenton, N. D.; Gerloch, M. *Int. Rev. Phys. Chem.* **1990**, *9*, 227.

Of course, we expect the effects of bond bending to be small. For each M−L ligation, we define a local frame with z directed from nickel to nitrogen and y normal to the Ni−N−C plane. The x axis lies in the Ni−N−C plane, directed from the nitrogen atom and into the chelate ring. Our CLF analysis of energies, intensities, and circular dichroism cannot support a full parameterization of these small bonding displacements. In any case, the gross uncertainty attached to the experimental magnitude of the rotatory strength renders a full analysis along these lines rather pointless. We have merely looked to see if the lower bound proposed by Harding et al.[10] *can* be reproduced within this scheme using a "normal" k value. We have investigated two models: one in which nonzero values of $e_{\sigma\pi x}$ and $e_{\pi x}$ characterize bent bonding in the local xz plane and one with $e_{\sigma\pi y}$ and $e_{\pi y}$ for misdirected valence in the yz plane. With k = 1.0, we find that the experimental CD spectrum can be reproduced quantitatively (together, of course, with the linearly polarized spectrum and the transition energies) using either $e_{\sigma\pi x}$ = 300 cm^{-1} with $e_{\pi x}$ = 30 cm^{-1} or $e_{\sigma\pi y}$ = −80 cm^{-1} with $e_{\pi y}$ = 30 cm^{-1}. The signs[28] of the $e_{\sigma\pi}$ parameters concur with the descriptions of likely bent bonding above.

Altogether then, parameters for bent bonding of only ca. 80−300 cm^{-1}, compared with e_σ of ca. 4000 cm^{-1}, are sufficient to decrease the calculated rotatory strength by a factor of about 4. Obviously we cannot differentiate between the two experimental measures[9,10] of rotatory strength in this chromophore, but we can reproduce either with *slightly* different parameterizations that accord with expectations of displaced electron density perfectly well.

Conclusions

From the outset, one would have expected the trisethylenediaminenickel(II) ion to provide a stringent test of any ligand-field model. The ligands are chemically symmetrical and the strict D_3 molecular symmetry establishes a single donor type. For this amine, only σ bonding is contemplated so that the ligand field is parameterized with just e_σ for energies and by just $^Pt_\sigma/^Ft_\sigma$ for intensities. So far as transition energies and intensity distributions in both linearly and circularly polarized spectra are concerned, experiment has been reproduced quantitatively and easily. The value e_σ = 4010 cm^{-1} is unexceptional and the four-to-one dominance of $^Pt_\sigma$ over $^Ft_\sigma$ accords well with both theory and experiment for a good donor ligand in which the bonding density is reasonably well polarized toward the metal. It is unfortunate that experiment has apparently failed to provide a sure measure of the absolute rotatory strengths for this chromophore. Even so, it has been possible to provide reasonable accounts of either experimental bound within perfectly sensible physical limits that alter the basic description very little.

Our original vibronic model, allowing free parameterization of all vibrational modes relative to each other and to the static contribution, was cumbersome and unsuccessful in defining a unique fit for this chromophore; it has been successful for several $CuCl_4^{2-}$ and PtX_4^{2-} (X = Cl, Br), however. But, our latest approach, in which vibronic analysis is predicated on detailed vibrational analysis, has made light of the problem.

Acknowledgment. A.J.B. and K.M.J. acknowledge awards of SERC Research Studentships.